Modeling of Solid-State Polymerization of Poly(ethylene terephthalate)

CHANG-KWON KANG

AspenTech Asia Ltd., 22/F, One Capital Place, 18 Luard Road, Wanchai, Hong Kong, People's Republic of China

Received 19 March 1997; accepted 27 August 1997

ABSTRACT: A mathematical model for solid-state polymerization of poly(ethylene terephthalate) was developed. The effects of temperature and chain entanglement on chain mobility were considered to estimate the rate constants of chemical reactions. The diffusivities of volatile byproducts could be determined using the free volume theory.[13,14] The model predictions were validated with experimental data reported in the literature. In addition, assuming that the concentration profiles of volatile byproducts in spherical particles are described by a sinusoidal function, the mass transfer rate of the byproducts at a given time could be derived as an ordinary differential equation that can be easily treated. © 1998 John Wiley & Sons, Inc. J Appl Polym Sci 68: 837–846, 1998

Key words: solid-state polymerization; poly(ethylene terephthalate)

INTRODUCTION

Solid-state polymerization (SSP) is an important process to synthesize high molecular weight poly(ethylene terephthalate) (PET) for injection or blow-molding applications. Generally, SSP is carried out by heating PET prepolymer to a temperature above its glass transition temperature but below its melting point. The two main reactions occurring during SSP are the esterification and the polycondensation. Volatile reaction byproducts, ethylene glycol (EG) and water, are released from the two reactions, and they are removed to enhance the forward reaction rate either by allowing a flow of inert gas or by applying vacuum.

Many efforts[1–9] have been made to investigate the mechanism of SSP. It has been clear that SSP depends not only on the chemical reactions but also on physical diffusion of the volatile byproducts through PET particles. Chen et al.[1] carried out the SSP for spherical particles with diameters of 0.097 and 0.213 cm at temperatures of 160, 180, and 200°C. In their study, the growth rate of molecular weight for small particles was found to be greater than that for large ones at 180 and 200°C. However, no influence of particle size on the variation of molecular weight were observed at 160°C. This might imply that the temperature dependence of chemical reaction rate is greater than that of diffusion rate of the volatile byproducts, and then the SSP is purely kinetically controlled at low temperatures.

This study is a continuation of the earlier works[10,11] pertaining to the modeling of PET polymerization process. The purpose here is to provide additional insight into the mechanism of SSP for improving the model predictability. Major parameters for the chemical reactions and physical diffusion occurring during SSP were estimated through model calculations. As a result, an explanation for the observation by Chen et al.[1] could be provided.

ASSUMPTIONS AND MODELING

Reaction Scheme

A modeling approach that properly accounts for varying chain lengths is required to establish a framework for representing polymer reaction ki-

Journal of Applied Polymer Science, Vol. 68, 837–846 (1998)
 CCC 0021-8995/98/050837-10

Table I Molecular Structures of Components Considered

Symbol	Descriptions	Molecular Structure
TPA	terephthalic acid	
EG	ethylene glycol	$HOCH_2CH_2OH$
W	water	H_2O
tEG	EG end group	$HOCH_2CH_2O\sim$
tTPA	TPA end group	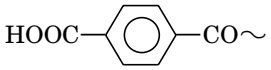
bEG	EG repeat unit	$\sim OCH_2CH_2O\sim$
bTPA	TPA repeat unit	
bDEG	diethylene glycol repeat unit	$\sim OCH_2CH_2OCH_2CH_2O\sim$
tVIN	vinyl end group	$CH_2{=}CHO\sim$
AA	acetaldehyde	CH_3CHO

netics. In this study, the polymer segment approach,[10–12] a functional group approach, was used to establish the overall reaction network. Polymerization reactions can be regarded as reactions between two functional groups. All components considered in the reaction scheme are listed in Table I, where six different oligomeric segments are defined: tEG, tTPA, tVIN, bEG, bTPA, and bDEG ("t" and "b" represent the terminal functional group and the bound monomer repeating unit, respectively).

The complete set of reactions considered here is shown in Table II. In this table, k_i ($i = 1–9$) are the rate constants and K_i ($i = 1–5$) are the equilibrium constants. Reactions 1–4 are the esterification reactions, and reaction 5 is the polycondensation reaction. Reaction 6 is a side reaction leading to the diethylene glycol (DEG) formation. Although several reaction mechanisms have been proposed to describe the DEG formation reaction, the mechanisms are lumped together in reaction 6. Reactions 7 and 8 are the thermal degradation reaction and the acetaldehyde formation reaction, respectively. Reaction 9 is the vinyl end-group consumption reaction.

Mass Balance Equations

During SSP, the unsteady-state diffusion of the volatile byproducts is coupled with the chemical reactions. The mass balance equation of volatile components in a spherical particle can be written as[6]

Table II Reaction Scheme Considered in This Work

		Rate Constants
No.	Reactions	Forward, Reverse
(1)	EG + TPA ⇄ tEG + tTPA + W	k_1, k_1/K_1
(2)	EG + tTPA ⇄ tEG + bTPA + W	k_2, k_2/K_2
(3)	tEG + TPA ⇄ bEG + tTPA + W	k_3, k_3/K_3
(4)	tEG + tTPA ⇄ bEG + bTPA + W	k_4, k_4/K_4
(5)	tEG + tEG ⇄ bEG + EG	k_5, k_5/K_5
(6)	tEG + tEG → bDEG + W	k_6, —
(7)	bEG + bTPA → tVIN + tTPA	k_7, —
(8)	tEG + bTPA → AA + tTPA	k_8, —
(9)	tEG + tVIN → bEG + AA	k_9, —

Table III $G_j(t)$ of Each Component

$G_{EG}(t) = -R_1 - R_2 + R_5$
$G_{TPA}(t) = -R_1 - R_3$
$G_{tEG}(t) = R_1 + R_2 - R_3 - R_4 - 2R_5 - 2R_6 - R_8 - R_9$
$G_{tTPA}(t) = R_1 - R_2 + R_3 - R_4 + R_7 + R_8$
$G_{bEG}(t) = R_3 + R_4 + R_5 - R_7 + R_9$
$G_{bTPA}(t) = R_2 + R_4 - R_7 - R_9$
$G_W(t) = R_1 + R_2 + R_3 + R_4 + R_6$
$G_{bDEG}(t) = R_6$
$G_{tVIN}(t) = R_7 - R_9$
$G_{AA}(t) = R_8 + R_9$

$$\frac{\partial C_j}{\partial t} = D_j\left[\frac{\partial^2 C_j}{\partial r^2} + \frac{2}{r}\frac{\partial C_j}{\partial r}\right] + G_j(t) \quad (\text{for } j = EG, W, \text{ and } AA) \quad (1)$$

where C_j is the concentration of component j; t, reaction time; D_j, the diffusion coefficient of volatile component j; and r, the distance from the origin of the sphere. On the other hand, the mass balance equation of nondiffusing components can be written as

$$\frac{dC_j}{dt} = G_j(t) \quad (j = \text{TPA, tEG, tTPA, bEG, bTPA, bDEG, and tVIN}) \quad (2)$$

In eqs. (1) and (2), $G_j(t)$ is the generation rate due to chemical reactions, and it can be expressed by a combination of the reaction rates, R_i ($i = 1$–9). $G_j(t)$ and R_i are listed in Tables III and IV, respectively.

In eq. (1), the diffusion process was assumed to be of Fickian type and isothermal without volume change of the particle. The relevant boundary and initial conditions for eq. (1) are as follows[6]:

$$C_j = C_j^S \quad \text{for } t > 0, \quad r = r_S \quad (3)$$

$$\frac{\partial C_j}{\partial r} = 0 \quad \text{for } t > 0, \quad r = 0 \quad (4)$$

$$C_j = C_j^0 \quad \text{for } t = 0, \quad 0 < r < r_S \quad (5)$$

where C_j^S and C_j^0 are the interfacial and the initial concentrations, respectively, and r_S is the radius of the sphere.

Diffusivity

In a recent modeling work, Devotta and Mashelkar[8] applied the free-volume theory[13,14] to diffusion of the volatile components occurring during SSP. According to the free-volume theory, the diffusivity of a diffusing small molecule in a very concentrated polymer solution can be given by[13,14]

$$D_j = RTA_j \exp\left[\frac{-B_j}{V_f}\right] \quad (\text{for } j = \text{EG, W, and AA}) \quad (6)$$

where A_j is the prefactor; B_j, the so-called jump factor of the diffusing component; V_f, the effective fractional free volume of the system; R, the gas constant; and T, the temperature in K. B_j depends on the size and shape of the diffusing molecule. The same values estimated by Kulkarni and Mashelkar[14] were used for determining B_j in our modeling.

V_f in eq. (6) can be given by[8]

$$V_f = f_A\Phi_A + f_{EG}\Phi_{EG} + f_W\Phi_W \quad (7)$$

Here, f_A, f_{EG}, and f_W denote the fractional free volumes of the amorphous phase, EG, and water, respectively, and Φ's are the volume fractions in the system. The contributions from the crystalline phase, the carrier gas used, and the other volatile byproducts (e.g., AA) were not considered in this equation. Also, f_A can be written by the following WLF equation[15]:

$$f_A = f_g + \alpha(T - T_g) \quad (8)$$

Table IV R_i of Each Reaction Listed in Table II

$$R_1 = 4k_1C_{EG}C_{TPA} - (k_1/K_1)C_WC_{tTPA}\frac{C_{tEG}}{C_{tEG} + C_{bEG}}$$

$$R_2 = 2k_2C_{EG}C_{tTPA} - 2(k_2/K_2)C_WC_{bTPA}\frac{C_{tEG}}{C_{tEG} + C_{bEG}}$$

$$R_3 = 2k_3C_{tEG}C_{TPA} - (k_3/K_3)C_WC_{tTPA}\frac{C_{bEG}}{C_{tEG} + C_{bEG}}$$

$$R_4 = k_4C_{tEG}C_{tTPA} - 2(k_4/K_4)C_WC_{bTPA}\frac{C_{bEG}}{C_{tEG} + C_{bEG}}$$

$$R_5 = k_5C_{tEG}C_{tEG} - 4(k_5/K_5)C_{EG}C_{bEG}$$

$$R_6 = k_6C_{tEG}C_{tEG}$$

$$R_7 = k_7C_{bEG}\frac{C_{bTPA}}{C_{tEG} + C_{bEG}}$$

$$R_8 = k_8C_{tEG}\frac{C_{bTPA}}{C_{tEG} + C_{bEG}}$$

$$R_9 = k_9C_{tEG}C_{tVIN}$$

where f_g is the fractional free volume at the glass transition temperature; α, the thermal expansion coefficient of the free volume; and T_g, the glass transition temperature of the polymer. For simplicity, the effect of molecular weight on T_g was not considered, although T_g may increase with molecular weight.

To determine Φ_A in eq. (7), the kinetics of isothermal crystallization[16] were considered, i.e.,

$$1 - \frac{\Phi_C}{\Phi_C^\infty} = \exp[-K_C t^n] \tag{9}$$

where Φ_C ($=1 - \Phi_A$) and Φ_C^∞ are the volume fractions of crystalline phase at a given time and at time of infinity, respectively; n, the Avrami exponent; and K_C, a coefficient depending on temperature and molecular weight. The experimental results found by Hartley et al.[17] were used for the estimation of K_C and n. The effect of molecular weight on the crystallization rate[16,18] was not considered.

Reaction Rate Constant

Above glass transition temperature, amorphous polymer chains have translational degrees of freedom. In comparison with the corresponding melt polymerization process, the chain mobility during SSP is relatively low, due to the low reaction temperature. The temperature dependence of chain mobility can be assumed to be of Arrhenius-type relationship, i.e.,

$$m_P \propto \exp\left[\frac{-E_P}{RT}\right] \tag{10}$$

where m_P is the chain mobility at a temperature, and E_P is the activation energy of translational motion.

The most prominent change occurring during SSP is the growth of polymer chains. It is well known that the translational mobility of polymer chains decreases with increasing their length, owing to the chain entanglement. According to the raptation theory[19] for considering the entanglement effect, the translational mobility of a raptating chain is inversely proportional to the square of the chain length, i.e.,

$$m_P \propto \frac{1}{X_n^2} \tag{11}$$

where X_n is the number-average degree of polymerization.

Hence, considering the reaction rate to be proportional to the chain mobility, the rate constant (k_i) between two reactive polymer chains can be mathematically expressed as follows:

$$k_i = A_i \frac{X_R^2}{X_n^2} \exp\left[\frac{-E_P}{RT}\right] \exp\left[\frac{-E_i}{RT}\right] \quad (i = 1\text{–}6 \text{ and } 9) \tag{12-1}$$

where A_i is the prefactor; X_R, the number-average degree of polymerization for a reference state; and E_i, the activation energy for reaction i. Because reactions 7 and 8 are intramolecular reactions not affected by the translational motion of polymer chains, the rate constant for them can be written as

$$k_i = A_i \exp\left[\frac{-E_i}{RT}\right] \quad (i = 7 \text{ and } 8) \tag{12-2}$$

Calculation

X_n of the polymer chains produced can be defined as

$$X_n = \frac{C_{\text{tEG}} + C_{\text{tTPA}} + C_{\text{bEG}} + C_{\text{bTPA}} + C_{\text{bDEG}} + C_{\text{tVIN}}}{C_{\text{tEG}} + C_{\text{tTPA}} + C_{\text{tVIN}}} \tag{13}$$

In trying to compare the calculated X_n with the corresponding experimental data of intrinsic viscosity (η), we used the following relationship[20]:

$$\eta = 2.1 \times 10^{-4} (192.17 \times X_n)^{0.82} \tag{14}$$

For solving the above mass balance equations, one must determine k_i ($i = 1\text{–}9$) and K_i ($i = 1\text{–}5$). As a first approximation, we assumed that $k_1 = k_2 = 0.5\ k_3 = 0.5\ k_4$, and $k_5 = k_9$.[21] Also, we used the same values reported in the literature for melt polymerization process with a single catalyst (Sb_2O_3),[21,22] except the prefactors for the two main reactions, i.e., A_3 and A_5. There is no reported experimental result for the chain mobility of solid-state PET in the open literature. In our model calculations, we used 13.5 kcal/mol for the value of E_P, which was determined from rheological data of molten PET.[23] Additionally, the mass transfer resistance in the gaseous phase was neglected and the concentration of volatile byprod-

Table V Numerical Values Used for the Calculation

(1) Overall

$B_{EG} = 0.070$; $B_W = 0.032$	eq. (6) ref. 14
$f_g = 0.025$; $\alpha = 4.5 \times 10^{-4}$ cm^3/K; $T_g = 337$ K	eq. (8) ref. 15, 24
$\Phi_C^\infty = 0.45$	eq. (9) —
$E_p = 13.5$ kcal/mol	eq. (10) ref. 23
$X_R = 100$	eq. (12) —

(2) Kinetic Parameters in Eq. (12) (refs. 21, 22)

Prefactor	Activation Energy	Equilibrium Constant
$A_1 = A_2 = 2\,A_3$	$E_1 = E_2 = E_3$	$K_1 = K_2 = 2.5$
$A_3 = A_4 = 6.8 \times 10^{12}$ (L/mol)/min	$E_3 = E_4 = 17.6$ kcal/mol	$K_3 = K_4 = 1.25$
$A_5 = 5.4 \times 10^{12}$ (L/mol)/min	$E_5 = 18.5$ kcal/mol	$K_5 = 0.50$
$A_6 = 1.8 \times 10^{15}$ (L/mol)/min	$E_6 = 29.8$ kcal/mol	—
$A_7 = 3.6 \times 10^9$ l/min	$E_7 = 37.8$ kcal/mol	—
$A_8 = 2.3 \times 10^9$ l/min	$E_8 = E_6$	—
$A_9 = A_5$	$E_9 = E_5$	—

(3) Adjusted Prefactors in the Diffusion Coefficient of eq. (8)

Component	A_j (cm^2/s)
EG	2.2×10^{-8}
Water	2.0×10^{-8}

A_3 and A_5 were adjusted against the experimental data of Chen and Chen.[5]

ucts at the surface was assumed to be zero (i.e., $C_j^S = 0$).

The numerical values used in the calculation are summarized at Table V. The numerical technique for solving the mass balance equations was a combination of the fourth Runge–Kutta method, which dealt with the time interval integration, and the finite difference method, which handled the integral divisions of the particle. The initial concentration of each component (C_j^0) in the prepolymer could be determined by referring to the measured data (e.g., η, carboxyl group content, and hydroxyl group content) provided in the reference. The initial concentrations of tEG, tTPA, bEG, and bTPA used in our model simulation were 0.0787, 0.0513, 7.0568, and 7.0842 mol/L, respectively. The initial concentrations of other components (i.e., EG, TPA, W, bDEG, tVIN, and AA) were assumed to be zero.

In the following section, we estimated the prefactors in the rate constants of the two main reactions (A_3 and A_5) and in the diffusivities of EG and water (A_{EG} and A_W) by fitting the model results against the published experimental data, η and carboxyl group content, of Chen and Chen.[5] The diffusivity of AA could not be estimated from the data fitting, because it does not affect both η and carboxyl group content of the polymer formed during SSP. Parameter estimation was carried out by means of a nonlinear least-squares method.

RESULTS AND DISCUSSION

Validation of Model

In Figure 1, the model results are fitted against four experimental data sets of Chen and Chen.[5] All the parameters adjusted here are listed in Table V. The model fits the experimental data very well, as shown at this figure. It is important to emphasize that no parameter for activation energy term (i.e., temperature dependence) has been adjusted. Better fitting results could be obtained if the value of E_P was also adjusted.

In Table VI, some values for the diffusivities and for the rate constants are compared with those obtainable from the reported data in the literature. It should be noted that the diffusivity values for EG and water obtained here are compa-

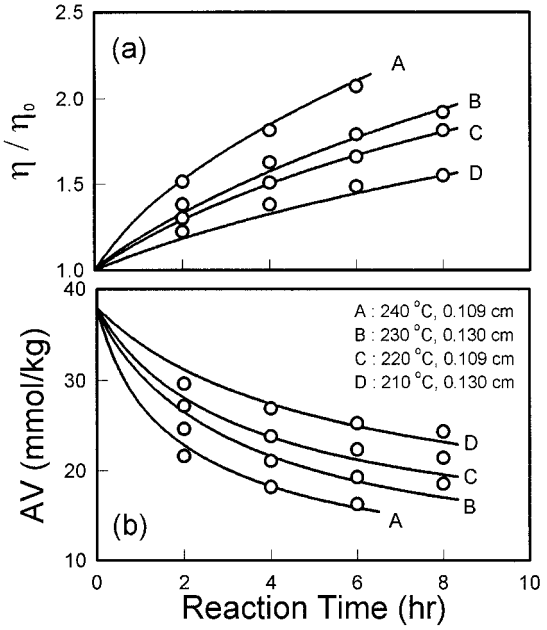

Figure 1 Estimation of the model parameters by fitting the model results against the experimental data of Chen and Chen[5]; (a) intrinsic viscosity, (b) carboxyl group content (AV). The solid lines are calculated by the model using the numerical parameters shown in Table V.

rable to those of the previous works. On the other hand, the values for the two rate constants obtained here are much larger than those found by Tang et al.[9] However, the direct comparison may not be quite reliable, because the rate constants depend on the reaction scheme considered and the amount of reaction catalysts[26] initially present at the prepolymer.

Because water diffuses from the interior of PET particles to the surface more easily than EG, the esterification reaction and water diffusion become dominant in the case of pellet-size particles with diameters of the order of 0.1 cm.[5,7] Therefore, it is important to note that the rate constant of the esterification reaction and the diffusivity of water might affect the results of model prediction more significantly.

Temperature Dependence of SSP

In Figure 2, the experimental data of Chen et al.[1] are compared with the model prediction. For the calculation, the same model parameters obtained from Figure 1 were used. The same initial conditions of Figure 1 were also used, because the exact values were not provided in the reference. From Figure 2 it is surprising to note that the model results closely fit the experimental data, even though the catalyst effect on the reaction rates was not taken into account and the exact values for the initial conditions were not used.

For estimating the diffusivities of EG and water, the same values of B_j estimated by Kulkarni and Mashelkar[15] were used. Then, the activation energies of EG and water diffusion used here were about 4.0 and 2.4 kcal/mol, respectively. There have been diversified values for the activation energy of EG diffusion reported in the literature, such as 31.3 kcal/mol by Ravindranath and Mashelkar[6] and 5.4 kcal/mol by Chen and Chen[5] (see Table VII). The major reason most likely to have given rise to this discrepancy is that the esterification reaction was not considered in the work of Ravindranath and Mashelkar.

As mentioned above, the observation by Chen et al.[1] implies that the temperature dependence of the chemical reaction rates should be greater than that of the diffusion (see Fig. 2). Moreover, many other experimental results has shown that the activation energies of the apparent rate constants for SSP are greater than those for the melt polymerization process, as seen at Table VII. In trying to explain this, we considered the temperature dependence of chain mobility (i.e., E_P) in the reaction rate expression. As a result, the activation energies of the apparent rate constants used here could become much larger than those of the diffusion of volatile components.

Effect of Crystallization

Figure 3 shows the effect of the crystallization on the growth rate of molecular weight (i.e., X_n). As predicted, the crystallization retards the growth rate. In industrial practice, copolymers containing a comonomer (e.g., isophthalic acid) are usually used as the prepolymer for SSP. The crystallization rate will be somewhat decreased due to the presence of the comonomer units.

Obviously, diffusion and reaction depend on the crystallization. However, the crystallization kinetics of eq. (9) may be not sufficient to predict the crystallinity, because the real situation is complicated with secondary crystallization, differences in core vs. surface crystallinity, nucleation of crystals by additives, etc. More elaborate experimental data will be required to take account into these phenomena in the modeling.

Chain Entanglement Effect

From experimental results, it seems likely that the overall rate of SSP decreases with time. There

Table VI Comparison with Other Studies

(1) Diffusion Coefficient at 230°C, cm^2/s

	EG	Water
This study	[a] 3.1×10^{-6}	[a] 5.7×10^{-6}
Ravindranath et al.[6]	[b] 3.6×10^{-6}	—
Tang et al.[9]	2.6×10^{-6}	5.8×10^{-6}
Schmalz et al.[25,27]	—	[c] 1.3×10^{-5}

[a] Calculated at $\Phi_C = 0.45$.
[b] Estimated from the Chang's data[2] without considering the esterification reaction.
[c] Deduced from extrapolation of the data obtained at 110–200°C.

(2) Reaction Rate Constant, (L/mol)/min

	Temperature	Esterification	Polycondensation
This study	230°C	[a] 5.3×10^{-2}	[a] 1.7×10^{-2}
	160°C		[b] 2.9×10^{-4}
Tang et al.[9]	230°C	1.1×10^{-2}	2.9×10^{-3}
Ravindranath et al.[6]	160°C	—	[c] 3.3×10^{-4}
Karayannids et al.[7]	230°C	—	[c] 1.8×10^{-2}

[a] Calculated at $X_n = 200$.
[b] Calculated at $X_n = 115$.
[c] Estimated using a purely kinetic model.

is room for argument on this point. In a previous work, Gaymans et al.[28] suggested that the distance of reactive end groups may be broadened during SSP and the reaction will be of end-group diffusion limiting. Further, Chen and Chen[5] developed a kinetic expression for end-group diffusion-limited reaction to explain their experimental results. On the other hand, Devotta and Mashelkar[8] assumed that there exists a sphere of action within which the reactive chain ends search for each other by a diffusional motion and the diffusivity of the end depends on the local free volume available in the polymeric media that decreases with reaction time. In this study, the chain entanglement effect was considered as a major factor decreasing the overall rate of SSP. This requires some further discussion.

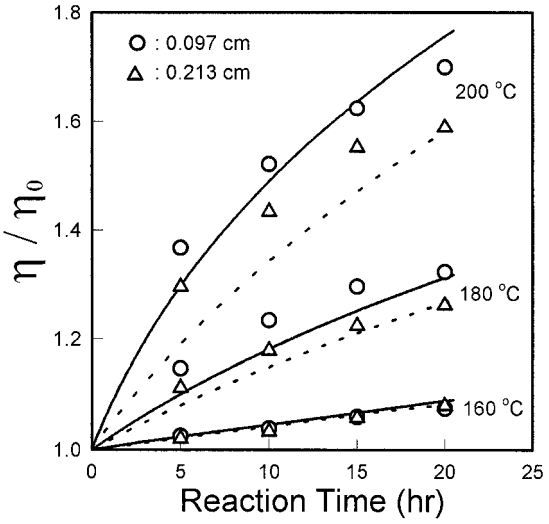

Figure 2 Comparison of the model prediction with the experimental data of Chen et al.[1] For the calculation, the same model parameters obtained from Figure 1 were used. The solid lines are calculated for particles with diameters of 0.097 cm, while the dotted ones are for 0.231 cm.

Mass Transfer Rate

In the unsteady-state mass transfer process, the concentration at a given position varies with time. In the case of SSP, however, the mass transfer rate at a given time is of greater interest than the concentration profile itself. First, we assume that the concentration profile of the volatile byproducts at time t is given by

$$C_j - C_j^S = f(r) = \frac{p}{r}\sin(\lambda r) + \frac{q}{r}\cos(\lambda r) \quad (j = \text{EG, W, and AA}) \quad (15)$$

Table VII Temperature Dependence

(1) Diffusion Coefficient, kcal/mol

	EG	Water
This study	4.0	2.4
Ravindranath et al.[6]	[a]31.3	—
Chen & Chen[5]	5.4	—
Schmalz et al.[25,27]	—	[b]8.7

[a] Estimated from the Chang's data[2] without considering the esterification reaction.
[b] Determined at temperatures 110–200°C.

(2) Reaction Rate Constant, kcal/mol

	Esterification	Polycondensation
This study	31.3 (=17.6 + 13.5)	32.0 (=18.5 + 13.5)
Chen and Chen[5]	19.1	24.0
Karayannids et al.[7]	[a]23.9	—
Kokkalas et al.[26]	26.0	[a]24.3
Yokoyama et al.[22]	[b]17.6	[b]18.5

[a] Estimated using a purely kinetic model.
[b] Determined from melt-phase polymerization.

where p, q, and λ are constants. Here, it should be noted that eq. (15) is a form of the mathematical solution for eq. (1) when there is no chemical reaction, i.e., $G_j(t) = 0$.[29] Because $G_j(t)$ is not a function of r, it may not affect the concentration profile significantly.

From the boundary conditions, $f(r)$ has to be finite at the origin and zero at the surface, i.e.,

$$f(r) = \frac{p}{r} \sin\left(\frac{\pi r}{r_S}\right) \tag{16}$$

Integrating eq. (16), p can be obtained as follows:

$$\int_0^{r_S} 4\pi r^2 \frac{p}{r} \sin\left(\frac{\pi r}{r_s}\right) dr = \frac{4}{3} \pi r_S^3 (C_j^{\mathrm{AVG}} - C_j^S) \tag{17}$$

where C_j^{AVG} is the average concentration of component j within the sphere. Then, one can obtain

$$f(r) = \frac{\pi}{3} (C_j^{\mathrm{AVG}} - C_j^S) \frac{r_S}{r} \sin\left(\frac{\pi r}{r_S}\right) \tag{18}$$

Now, the transfer rate per unit volume across the surface of sphere, $N_j(t)$, is

$$N_j(t) = -\frac{3}{r_S} D_j \left.\frac{\partial f(r)}{\partial r}\right|_{r=r_S} = \frac{\pi^2 D_j}{r_S^2} (C_j^{\mathrm{AVG}} - C_j^S) \tag{19}$$

Consequently, the mass balance equation of the diffusing components can be written as

$$\frac{dC_j}{dt} = N_j(t) + G_j(t) = \frac{\pi^2 D_j}{r_S^2} (C_j - C_j^S) + G_j(t) \quad (j = \text{EG, W, and AA}) \tag{20}$$

Equation (20) is of the ordinary differential type, which is more easily treated than eq. (1). Here, the validity of eq. (15), which is the only assumption used for deriving eq. (20), should be mentioned. Figure 3 shows the concentration profiles for EG calculated from eq. (1). From this figure, it seems likely that the profile can be described by a sinusoidal form of eq. (15). In Figure 4, the calculated X_n by eq. (20) are compared with those by eq. (1). It can be clearly shown that there is no detectable discrepancy between the two calculated results. Accordingly, it seems reasonable to suppose that eq. (20) is valid for the mass bal-

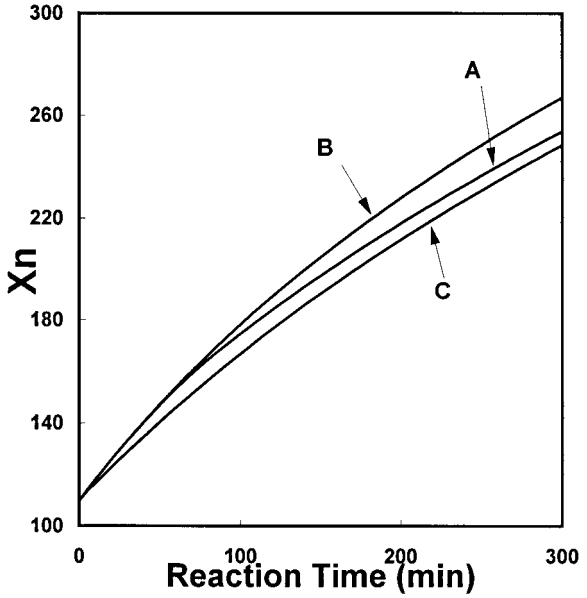

Figure 3 Effect of crystallization on the chain growth rate. For the calculation, it was assumed that the reaction temperature is 240°C and the diameter of particles is 0.109 cm. The same model parameters, except for the crystallization kinetics obtained from Figure 1, were used. For the calculation of curve A, it was assumed that K_C and n are 5.1×10^{-8} and 4, respectively. For curves B and C, the crystallization rates were assumed to be zero and infinity, respectively.

ance equation of the volatile byproducts formed during SSP. Furthermore, the equation is very useful to save the calculation time effectively.

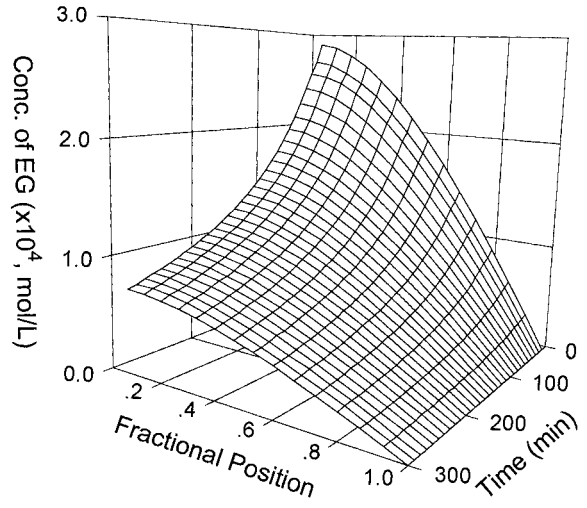

Figure 4 Internal distribution of EG in a spherical pellet with diameter of 0.130 cm during SSP at 230°C. The same model parameters obtained from Figure 1 were used.

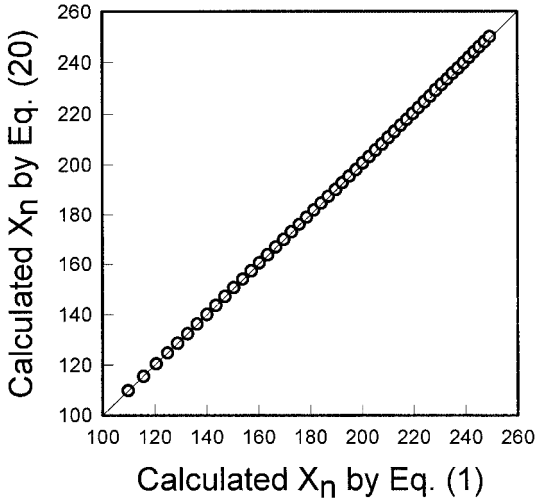

Figure 5 Comparison of the calculated results by eq. (20) with those by eq. (1). The same model parameters obtained from Figure 1 were used. The diameter of the particle and the reaction temperature were assumed to be 0.130 cm and 230°C, respectively. The solid line represents the ideal case where the calculated X_n by eq. (20) are exactly equal to those by eq. (1). The distance between the plotted points and this line indicates the absolute error between the two calculated results.

NOTATION

A_i, A_j: prefactors in eqs. (12) and (6), respectively
B_j: jump factor of volatile component j in eq. (6)
C_j: concentration of component j (mol/L)
C_j^{AVG}: average concentration of volatile component j within sphere
C_j^S: concentration of volatile component j at surface of sphere
C_j^0: initial concentration of component j
D_j: diffusivity of volatile component j (cm^2/s)
E_i: activation energy for reaction i (i = 1–6)
E_P: activation energy for chain mobility
f_A: fractional free volume of amorphous phase
f_{EG}: fractional free volume of EG
f_g: fractional free volume at T_g
f_W: fractional free volume of water
$f(r)$: concentration profile of volatile component, defined as eq. (15)
$G_j(t)$: generation rate of component j due to chemical reactions
j: component, defined in Table I
K_C: coefficient in eq. (9)

K_i: equilibrium constant for reaction i (i = 1–5)
k_i: rate constant (L/mol·min) for reaction i (i = 1–9)
m_P: chain mobility, defined as eq. (10)
n: Avrami exponent in eq. (9)
$N_j(t)$: mass transfer rate of volatile component j, defined as eq. (19)
p, q: constants in eq. (15)
R: gas constant
R_i: reaction rate for reaction i (i = 1–9)
r: distance from origin of sphere
r_S: radius of sphere
T: reaction temperature (K)
T_g: glass transition temperature of polymer (K)
t: reaction time
V_f: effective fractional free volume of system, defined as eq. (7)
X_n: number average degree of polymerization, defined as eq. (13)
X_R: X_n at reference state

Greek Letters

α: thermal expansion coefficient of free volume (cm^3/K)
η: intrinsic viscosity of polymer
η_O: intrinsic viscosity of prepolymer
λ: constant in eq. (15)
Φ_A: volume fraction of amorphous phase
Φ_C: volume fraction of crystalline phase
Φ_C^∞: maximum volume fraction of crystalline phase
Φ_{EG}: volume fraction of EG
Φ_W: volume fraction of water

REFERENCES

1. F. C. Chen, R. G. Griskey, and G. H. Beyer, *AIChE J.,* **15,** 680 (1969).
2. T. M. Chang, *Polym. Eng. Sci.,* **10,** 364 (1970).
3. S. Chang, M.-F. Sheu, and S.-M. Chen, *J. Appl. Polym. Sci.,* **28,** 3289 (1983).
4. S. A. Jabarin and E. A. Lofren, *J. Appl. Polym. Sci.,* **32,** 5315 (1986).
5. S. Chen and F. Chen, *J. Polym. Sci., Polym. Chem. Ed.,* **25,** 533 (1987).
6. K. Ravindranath and R. A. Mashelkar, *J. Appl. Polym. Sci.,* **39,** 1325 (1990).
7. G. Karayannidis, I. Sideridou, D. Zamboulis, G. Stalidis, D. Bikiaris, N. Lazaridis, and A. Wilmes, *Angew. Makromol. Chem.,* **192,** 155 (1991).
8. I. Devotta and R. A. Mashelkar, *Chem. Eng. Sci.,* **48,** 1859 (1993).
9. Z.-L. Tang, N.-X. Huang, and C. Sironi, *J. Appl. Polym. Sci.,* **57,** 473 (1995).
10. C. -K. Kang, B. C. Lee, and D. W. Ihm, *J. Appl. Polym. Sci.,* **60,** 2007 (1996).
11. C.-K. Kang, B. C. Lee, D. W. Ihm, and D. A. Tremblay, *J. Appl. Polym. Sci.,* **63,** 164 (1997).
12. T. L. Mock, C.-C. Chen, D. L. Phipps, Jr., and R. A. Greenberg, AIChE Spring National Meeting, 1988.
13. M. H. Cohen and D. Turnbull, *J. Chem. Phys.,* **31,** 1164 (1959).
14. M. G. Kulkarni and R. A. Mashelkar, *Chem. Eng. Sci.,* **38,** 925 (1983).
15. M. L. Williams, R. F. Landel, and J. D. Ferry, *J. Am. Chem. Soc.,* **77,** 3701 (1955).
16. B. Wunderlich, *Macromolecular Physics,* Vol. 2, Academic Press Inc., New York, 1980.
17. F. D. Hartley, F. W. Lord, and L. B. Morgan, *Philos. Trans. R. Soc. Lond.,* **A247,** 23 (1954).
18. F. van Antwerpen and D. W. van Krevelen, *J. Polym. Sci., Polym. Phys. Ed.,* **10,** 2423 (1972).
19. P. G. de Gennes, *Scaling Concepts in Polymer Physics,* Cornell University Press, Ithaca, New York, 1979, p. 227.
20. A. Conix, *Makromol. Chem.,* **26,** 226 (1958).
21. K. Ravindranath and R. A. Mashelkar, *Polym. Eng. Sci.,* **22,** 619 (1982).
22. H. Yokoyama, J. Sano, T. Chijiiwa, and R. Kajiya, *J. Jpn. Petrol. Inst.,* **21,** 271 (1978).
23. D. R. Gregory, *J. Appl. Polym. Sci.,* **16,** 1479 (1972).
24. W. Wrasidlo, *Themal Analaysis of Polymer, Advances in Polymer Science,* Vol. 13, Springer-Verlag, New York, 1974, p. 3.
25. E. O. Schmalz and H. Grundke, *Textiletechnology,* **20,** 456 (1969).
26. D. E. Kokkalas, D. N. Bikiaris, and G. P. Karayannidis, *J. Appl. Polym. Sci.,* **55,** 787 (1995).
27. B. D. Whitehead, *Ind. Eng. Chem. Process Des. Dev.,* **16,** 341 (1977).
28. R. J. Gaymans, J. Amirtharaj, and H. Kamp, *J. Appl. Polym. Sci.,* **27,** 2513 (1982).
29. A. H. P. Skelland, *Diffusional Mass Transfer,* Wiley, New York, 1974, p. 21.